RSC Mechanochemistry

ROYAL SOCIETY OF CHEMISTRY

PAPER

View Article Online
View Journal



Cite this: DOI: 10.1039/d5mr00161g

# Amorphous-to-crystalline transformation: a mechanochemical pathway to imine-linked covalent organic frameworks

Normanda Brown,[a] Yogendra Nailwal,[a] Tyra Blair,[a] Ziad Alsudairy,[b] Qingsong Zhang,[c] Krystal Kennedy,[a] Yi Liu[c] and Xinle Li*[a]

Received 26th December 2025
Accepted 28th January 2026

DOI: 10.1039/d5mr00161g

rsc.li/RSCMechanochem

Amorphous-to-crystalline transformation is of profound importance in the crystallization of covalent organic frameworks (COFs), yet its potential through solid-state mechanochemistry remains largely unexplored. Here, we introduce a mechanochemical amorphous-to-crystalline pathway to synthesize imine-linked COFs under ambient conditions. By ball milling their amorphous progenitors, nine imine-linked COFs with distinct core structures, topologies (**hcb**, **sql**, **kgm**, and **dia**), and dimensions are constructed in as little as one hour. Notably, the unique advantage of this method is highlighted by the successful synthesis of a highly crystalline, porous pyrene-based COF inaccessible by *de novo* mechanosynthesis. A mechanochemical "scrambling" reaction of imine-based model compounds confirms the high reversibility of the imine bonds in the solid state, which is crucial for facilitating error correction during COF reconstruction. This study underscores mechanochemistry as an effective means for amorphous-to-crystalline transformation, establishing a facile, generic, and green pathway to imine-linked COFs, including those unattainable *via* conventional *de novo* mechanosynthesis.



## Introduction

Covalent organic frameworks (COFs) are frontier reticular materials constructed by precisely integrating discrete organic monomers into crystalline one-, two-, and three-dimensional (1D, 2D, and 3D) extended networks.[1] Characterized by their exceptional structural merits, such as low density, high porosity, ordered skeletons, diverse topologies, and modular functionalities, COFs have been in the limelight of porous materials research with widespread applications, including gas separation,[2] sensing,[3] energy storage,[4] biomedicine,[5] environmental remediation,[6] water harvesting,[7] and catalysis.[8] The formation of COFs is typically governed by the principles of dynamic covalent chemistry (DCC),[9] wherein reversible covalent bonds dynamically break and reform to repair the amorphous networks, ultimately yielding the most thermodynamically stable crystalline materials.[10] Consequently, this amorphous-to-crystalline transformation plays a pivotal role in COF crystallization and provides unambiguous evidence for DCC in this process.[11] In recent years, this unique feature has been strategically leveraged for the synthesis of COFs, enriching the synthetic toolbox for COFs.[12–15] For instance, in 2016, Tan *et al.* exploited the disorder-to-order reformation to synthesize $Fe_3O_4$@COF microspheres, which displayed a unique near-infrared photothermal conversion ability.[16] Similarly, in 2022, Xiong *et al.* employed the amorphous-to-crystalline transformation to fabricate a library of hollow COFs.[17] Beyond powdered COFs, in 2021, Fan *et al.* extended this strategy to the synthesis of COF membranes from amorphous precursors *via* monomer exchange, resolving hurdles associated with powder processability and membrane scalability.[18] Most recently, in 2025, Cusin *et al.* developed free-standing micrometer-thick 2D COF films by converting the pre-aligned amorphous 3D covalent adaptable network into crystalline products.[19] Despite significant progress, the amorphous-to-crystalline transformation is predominantly performed under solvothermal conditions, which are fraught with major limitations, including high energy consumption, multi-day reaction time, usage of environmentally harmful solvents, and cumbersome degassing protocols.[20] Therefore, there remains a pressing need to develop facile, rapid, and environmentally benign synthetic protocols for amorphous-to-crystalline transformation in COFs.

Mechanochemistry, a new branch of chemistry that induces chemical reactions through sustained mechanical force, has emerged as an appealing alternative to traditional solution-based methods.[21] Capitalizing on its unique advantages, including low carbon footprint, high efficiency, operation simplicity, and exceptional scalability, mechanochemistry has found broad applications across diverse material classes, such

[a]*Department of Chemistry, Clark Atlanta University, Atlanta, Georgia 30314, USA. E-mail: xli1@cau.edu*

[b]*Department of Chemistry, College of Science, Qassim University, Buraidah, 51452, Saudi Arabia*

[c]*The Molecular Foundry, Lawrence Berkeley National Laboratory, Berkeley, California 94720, USA*

as organic molecules,[22] nanomaterials,[23] organometallic compounds,[24] polymers,[25] porous materials,[26] and metal–organic frameworks (MOFs).[27] The first mechanosynthesis of COFs was demonstrated by Banerjee's group in 2013, when they made three β-ketoenamine-linked COFs *via* manual grinding.[28] Since then, the field of COF mechanochemistry has garnered increasing attention, with remarkable advances in the solid-state synthesis of various COFs and hybrid composites.[29–34] Beyond sustainability and environmental benignity in comparison to solution-based approaches, mechanochemistry offers the potential to produce COFs with exceptional material properties, such as enhanced surface area compared to their solvothermal counterparts.[35–37] More intriguingly, mechanochemistry can even enable the synthesis of COFs that are challenging to obtain in solution.[38] Despite considerable strides in the *de novo* mechanosynthesis of COFs, harnessing mechanochemistry for the synthesis of COFs from their amorphous counterparts remains largely unexplored.[39] Keeping these in mind, we envision that mechanochemistry can induce solid-state amorphous-to-crystalline transformation in COFs, thereby expanding the synthetic toolkit of COF mechanochemistry.

In this study, we report a mechanochemical strategy for synthesizing various imine-linked COFs from their amorphous progenitors *via* solid-state amorphous-to-crystalline transformation (Scheme 1). Employing ball milling under ambient conditions, we successfully obtained a broad range of imine COFs featuring diverse pore surfaces, skeleton flexibility, topologies (**hcb**, **sql**, **kgm**), and dimensions (2D and 3D) within an hour. The successful amorphous-to-crystalline transformation in one representative 2D COF was unambiguously confirmed by PXRD analysis, $N_2$ sorption measurement, and TEM imaging. Remarkably, this strategy enabled the synthesis of a pyrene-based rhombic COF that was inaccessible by *de novo* mechanosynthesis, highlighting the unique advantage of this approach. To gain mechanistic insight into mechanochemical transformation, a scrambling model reaction was conducted under ball-milling conditions, unequivocally confirming the high reversibility of the imine bonds in the solid state.

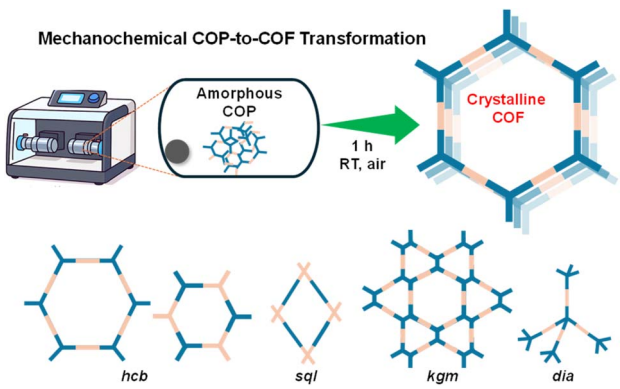


Scheme 1 Mechanochemistry enables efficient amorphous-to-crystalline transformation, yielding imine-linked COFs with diverse topologies (**hcb**, **sql**, **kgm**, and **dia**) from their amorphous progenitors under ambient conditions within an hour.

## Results and discussion

We commenced our study by synthesizing a 2D imine-linked COF, DBrTP-TPB,[40] which consisted of 2,5-dibromobenzene-1,4-dicarboxaldehyde (DBrTP) and 1,3,5-tris(4-aminophenyl) benzene (TPB), through the mechanochemical transformation of its amorphous progenitor (Fig. 1A). This route involves two steps: (1) the room temperature synthesis of amorphous covalent organic polymer (COP) *via* Schiff-base reaction of DBrTP and TPB, and (2) the subsequent ball milling of COP with a catalytic amount of Brønsted acid and liquid additive in a Retsch MM400 mill under ambient conditions. Amorphous COP was readily obtained with a nearly quantitative yield, and its disordered nature was verified by the featureless powder X-ray diffraction (PXRD) pattern (Fig. S1). Strikingly, crystalline COF was obtained within one hour of milling, as evidenced by the emergence of strong peaks in its PXRD pattern (Fig. 1). This finding validates the feasibility of using mechanochemistry to induce amorphous-to-crystalline transformation in COFs.

To further enhance the crystallinity of the obtained DBrTP-TPB COF, we systematically optimized key synthetic parameters influencing the mechanochemical COP-to-COF transformation, including catalyst, liquid additives, ball size, milling frequency, and milling time. We first investigated the effect of Brønsted acid catalysts. Among the tested acids, 6 M trifluoroacetic acid (TFA) proved optimal, yielding the highest crystallinity compared to pure TFA and glacial acetic acid (Fig. 1B). In addition, the presence of liquid additives significantly enhanced the crystallinity of COFs. *N*,*N*-dimethylacetamide (DMAc) was found to be optimal, outperforming acetonitrile, mesitylene, 1,4-dioxane, 1,2-dichlorobenzene (DCB), *N*,*N*-dimethylformamide (DMF), and *n*-butanol, which all resulted in amorphous products (Fig. 1C). Both liquid additives and catalysts were indispensable for the amorphous-to-crystalline transformation, as milling COPs without them did not yield any crystalline COFs (Fig. S1). Interestingly, the steel ball size also influenced the crystallinity,

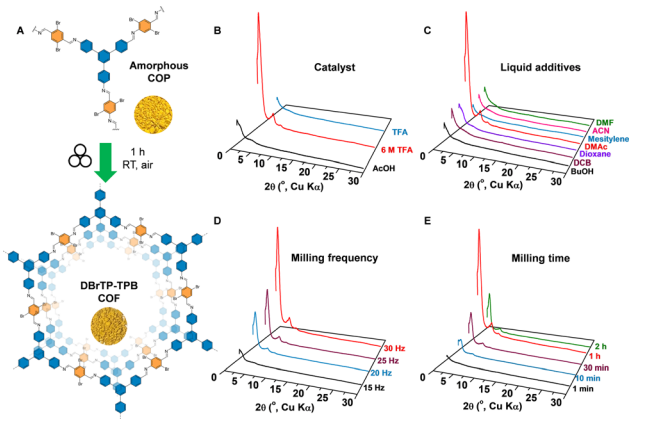


Fig. 1 (A) Schematic of mechanochemical transformaiton of amorphous COP into DBrTP-TPB COF. PXRD patterns of DBrTP-TPB obtained from ball milling its COP precursor with variations in (B) acid catalyst, (C) liquid additives, (D) milling frequencies, and (E) milling time.

with a 5 mm ball yielding the highest crystallinity compared to 7 mm and 10 mm balls (Fig. S2). Moreover, the effect of milling frequency on the crystallinity of COF was also examined. Increasing the milling frequency from 15 to 30 Hz enhanced the crystallinity of the resultant COF (Fig. 1D). To gain further insight into the transformation process, a time-resolved *ex situ* PXRD study was conducted. Crystalline features of DBrTP-TPB emerged after milling of COP for 10 minutes, and the crystallinity progressively increased with extended milling, reaching the maximum at 1 h. However, prolonged milling for 2 h decreased the crystallinity of COF (Fig. 1E). Ultimately, highly crystalline DBrTP-TPB was obtained with a yield of 70% by ball milling its COP precursor (40 mg) using DMAc (20 μL) as the liquid additive, 6 M TFA (15 μL) as the catalyst ($\eta$ = 0.88 μL mg$^{-1}$, where $\eta$ is the ratio of the liquid volume to the reactant mass), and one 5 mm steel ball at a milling frequency of 30 Hz for 1 h. The moderate yield is presumably due to material loss and partial decomposition of amorphous networks into oligomers that are subsequently removed during the workup process. Scalability, a crucial factor for the potential industrialization of COFs,[41] was assessed by scaling up the reaction to a gram scale using a 25 mL milling jar. Gratifyingly, the amorphous-to-crystalline transformation proceeded smoothly in the large state, affording *ca.* 0.5 g of highly crystalline DBrTP-TPB, with crystallinity comparable to the small-scale synthesis (Fig. S3). This finding highlights the practical applicability and scalability of the mechanochemical COP-to-COF transformation.

The chemical structures, crystallinity, porosity, morphology, and thermal stability of the resulting DBrTP-TPB were thoroughly characterized. Fourier transform infrared (FTIR) spectra of COP and DBrTP-TPB are similar, both showing characteristic C=N stretch at 1620 cm$^{-1}$, accompanied by the attenuation of the CHO stretch (1682 cm$^{-1}$) of DBrTP and N–H stretch (3354 cm$^{-1}$) of TPB (Fig. S4 and S5), suggesting the retention of chemical integrity after the mechanochemical transformation. The crystallinity of both materials was assessed by PXRD analysis. COP revealed a featureless PXRD pattern, substantiating its amorphous nature (Fig. 2A, black curve). In stark contrast, DBrTP-TPB exhibited high crystallinity with a sharp diffraction peak at $2\theta = 2.8°$ and several minor peaks at 5.2°, 5.7°, 7.6°, and 25.4° (Fig. 2A, red curve), corresponding to the (100), (110), (200), (210), and (001) facets, respectively. In addition, this experimental PXRD pattern is in line with the simulated one based on the eclipse stacking mode in previously reported literature.[42] The permanent porosity of both COF and COP samples was investigated by nitrogen sorption analysis at 77 K (Fig. 2B and S6). DBrTP-TPB displayed a type-IV sorption isotherm, characteristic of mesoporous materials. The Brunauer–Emmett–Teller (BET) surface area of DBrTP-TPB was calculated to be 848 m$^2$ g$^{-1}$, representing a more than 10-fold increase compared to the COP (65 m$^2$ g$^{-1}$). Furthermore, its pore size distribution simulated by nonlocal density functional theory (NLDFT) revealed a narrow pore width centered around 3.2 nm (Fig. 2B, inset), in good agreement with the theoretical value.[42] Thermogravimetric analysis (TGA) indicated that DBrTP-TPB possessed high thermal stability up to ~400 °C

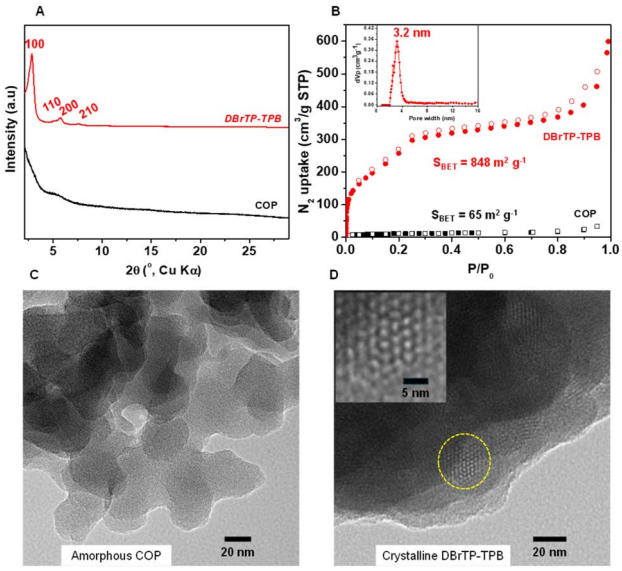


Fig. 2 (A) PXRD patterns of DBrTP-TPB COF and its amorphous COP precursor; (B) nitrogen adsorption–desorption isotherms. Inset is the pore size distribution of DBrTP-TPB COF; TEM images of (C) COP precursor and (D) DBrTP-TPB COF. The inset image shows the hexagonal pore structure.

under nitrogen (Fig. S7). Noteworthy, the successful amorphous-to-crystalline transformation was corroborated by transmission electron microscopy (TEM) images. The amorphous COP exhibited a ~50 nm size without noticeable ordered fringes (Fig. 2C). Upon mechanochemical transformation, the resulting DBrTP-TPB showed ordered hexagonal pores of ~3 nm across many regions (Fig. 2D, inset and S8). The significant visual difference in the TEM images, coupled with the pronounced enhancement in crystallinity and porosity, collectively confirms that mechanochemistry effectively drives the transformation of amorphous polyimines into well-ordered, highly crystalline COFs.

The efficient mechanochemical COP-to-COF transformation in the solid state prompted us to elucidate the underlying mechanism. We hypothesized that the reversibility of imine bonds under mechanical force dictates this structural reorganization. To verify this, we conducted a mechanochemical "scrambling" reaction using a molecular model compound, a strategy that has long been used to probe the dynamic nature of covalent bonds.[43] Specifically, an imine molecular analog, Br-TFPB-imine, was ball-milled with *p*-anisidine in the presence of a catalytic amount of acetic acid and ethanol as the liquid additive (Fig. 3A). Solution $^1$H NMR analysis revealed that the mechanochemical "scrambling" reaction proceeded efficiently under ambient conditions, yielding the exchanged product (OMe-TFPB-imine, red curve in Fig. 3B) in a nearly quantitative yield after just 10 minutes of milling at 20 Hz. These findings unambiguously confirm the highly dynamic nature of imine bonds in the solid state under mechanical force, which is pivotal for the error correction during the mechanochemical COP-to-COF transformation. By combining insights from the scrambling experiment with *ex situ* PXRD analysis, we postulate

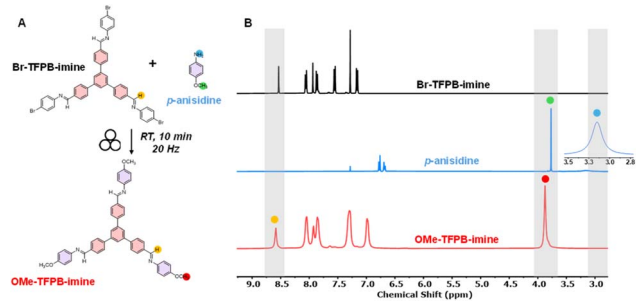


Fig. 3 (A) Scrambling reaction of molecular model compound, Br-TFPB-imine, and *p*-anisidine to yield OMe-TFPB-imine under ball milling; (B) $^{1}$H NMR spectra ($CDCl_3$, 298 K) of Br-TFPB-imine (black), *p*-anisidine (blue), and OMe-TFPB-imine (red).

a plausible mechanochemical pathway for the amorphous-to-crystalline transformation. During automated ball milling, sustained contact between the COP and the milling media enables the efficient dynamic breaking and reforming of imine bonds under catalytic conditions and in the presence of a liquid additive. This continuous bond reformation effectively "heals" the amorphous material, rapidly driving the disordered network toward the most thermodynamically most stable crystalline product.

The mechanochemical COP-to-COF transformation strategy is broadly applicable to a wide range of literature-known COFs encompassing various pore surfaces, shapes, and dimensionalities (Fig. 4). The detailed synthetic protocols and extensive optimization conditions are summarized in the SI (Tables S1–S6 and Fig. S9–S15). In total, nine highly crystalline imine-linked COFs were obtained from their COP precursors within as little as one hour under ambient conditions. PXRD verified their crystalline structures, and the resulting diffraction patterns closely matched previously reported data. This method proved effective for COFs with varied pore sizes (micro-to-meso pores) and core functionalities, including halogens (DBrTP-TPB,[40] and TFTP-TPB,[44] Fig. 4A and B), triazines (DMTP-TTA,[45] Fig. 4C), methyl (TFB-BD-Me,[46] Fig. 4D), and tertiary amines (TFPT-TAPT,[47] Fig. 4E). In addition to COFs typically constructed from rigid monomers, this strategy was also applicable to a flexible triazine-cored 2D COF, TPT-CHO-BD-OMe,[38] comprising 4,6-tris(4-formylphenoxy)-1,3,5-triazine (TPT-CHO) and o-dianisidine (BD-OMe) (Fig. 4F). Furthermore, the strategy accommodates different topologies (**hcb**, **sql**, and **kgm**) arising from $[C_3 + C_2]$, $[C_3 + C_3]$, and $[C_2 + C_2]$ combinations, yielding

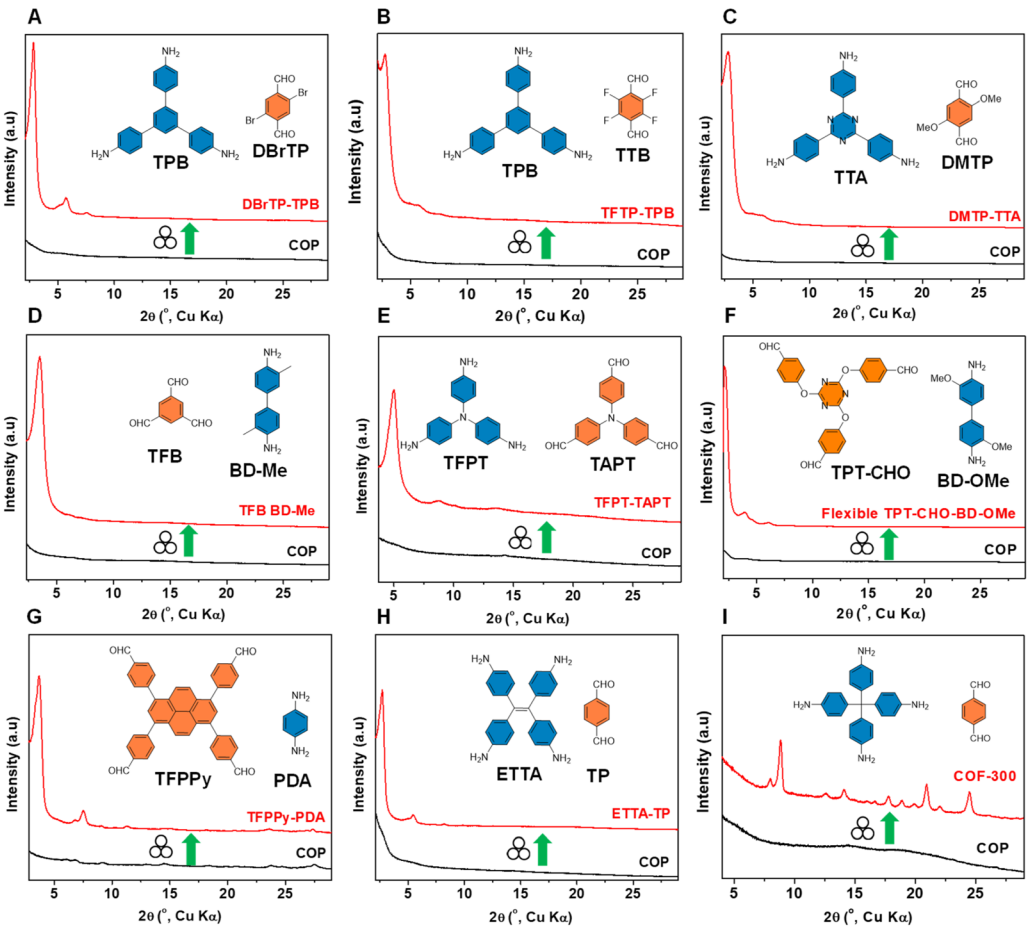


Fig. 4 Applicability of the mechanochemical COP-to-COF transformation within an hour under ambient conditions. PXRD patterns of (A) DBrTP-TPB;[40] (B) TFTP-TPB;[44] (C) DMTP-TTA;[45] (D) TFB-BD-Me;[46] (E) TFPT-TAPT;[47] (F) TPT-CHO-BD-OMe;[38] (G) TFPPy-PDA;[48] (H) ETTA-TP;[49] (I) COF-300.[50]

hexagonal (Fig. 4A–F), rhombic (TFPPy-PDA,[48] Fig. 4G), and dual-pore Kagome 2D COFs (ETTA-TP,[49] Fig. 4H). It is noteworthy that hexagonal COFs are most commonly studied in COF mechanochemistry, whereas alternative topologies remain minimally explored.[51] This strategy thus expands the topological diversity of COFs obtained through mechanochemistry. In addition to the dominant 2D architecture, this strategy also enabled the synthesis of an iconic 3D COF, COF-300 (Fig. 4I),[50] further highlighting its versatility. Taken together, this mechanochemical COP-to-COF transformation strategy exhibits excellent generality and efficiency for the rapid synthesis of imine-linked COFs from their amorphous counterparts under ambient conditions. Given the vast structural diversity of COPs with reversible linkages, we anticipate that this method holds considerable promise for expanding the structural diversity of COFs. Furthermore, it can regenerate COFs that become structurally flawed during use, consequently restoring their function and extending their effective lifespan in niche applications such as catalysis, energy storage, and remediation.

Beyond its synthetic ease, efficiency, scalability, generality, and sustainability, the mechanochemical transformation strategy offers an additional advantage by enabling the synthesis of COFs inaccessible *via de novo* mechanosynthesis. As a proof-of-concept, a rhombic pyrene-based imine-linked COF, TFPPy-PDA (Fig. 5), was selected for its unique properties and uncharted mechanosynthesis. The *de novo* mechanosynthesis of TFPPy-PDA was conducted by ball milling 1,3,6,8-tetrakis(4-formylphenyl)pyrene (TFPPy) and *p*-phenylenediamine (PDA) in the presence of liquid additives and an acid catalyst under ambient conditions. Despite exhaustive screening of reaction parameters, including liquid additives (up to eight), acid catalysts (AcOH, 6 M TFA, 9 M TFA, and TFA), milling frequency (20 Hz and 30 Hz), and milling materials (stainless steel and $ZrO_2$) (Table S7), crystalline frameworks were not obtained with low-to-moderate yields. Moreover, the unreacted TFPPy monomer still existed after mechanosynthesis (Fig. S16). In stark contrast, highly crystalline TFPPy-PDA was successfully obtained using the mechanochemical transformation strategy, wherein the COP was milled in the presence of 1,4-dioxane and 6 M TFA at 30 Hz for one hour. The PXRD pattern of the resulting TFPPy-PDA displayed an intense diffraction peak at $2\theta = 3.7°$, along with minor peaks at 6.7°, 7.5°, and 11.3° (Fig. 5A, red curve), corresponding to the (110), (210), (220), and (240) facets, respectively, consistent with the previous literature.[48] Furthermore, nitrogen sorption analysis revealed that mechanochemically transformed TFPPy-PDA exhibited a high BET surface area of 850 $m^2\ g^{-1}$, significantly exceeding that (150 $m^2\ g^{-1}$) of its counterpart made using *de novo* mechanosynthesis (Fig. 5B). By enabling access to COFs that are otherwise hard to obtain through conventional *de novo* mechanosynthesis, this mechanochemical transformation strategy complements and expands the existing synthetic toolkit of COF mechanochemistry. We attribute this difference to the distinct reaction pathways: in the *de novo* synthesis, the COF formation likely proceeds through the initial polymerization, resulting in an amorphous COP intermediate that subsequently undergoes a slow disorder-to-order reformation.[11] For the TFPPy-PDA system, the initial polymerization under ball milling is inefficient, thereby hindering subsequent crystallization. In contrast, mechanochemical transformation bypasses the initial amorphization stage and directly reconstructs the pre-formed COP into a crystalline framework by capitalizing on the high reversibility of imine bonds in the solid state, leading to the rapid formation of high-quality COFs.

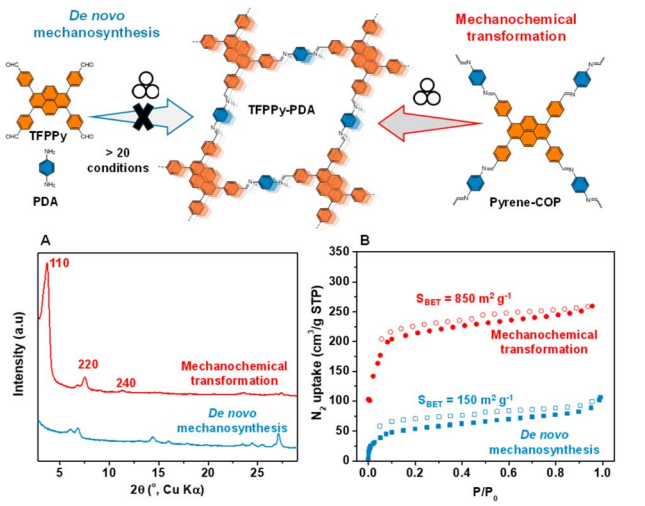


Fig. 5 Comparison of the synthesis of TFPPy-PDA through the *de novo* mechanosynthesis (left) and mechanochemical COP-to-COF transformation strategy (right). (A) PXRD patterns, and (B) nitrogen sorption isotherms.

## Conclusions

In conclusion, we have developed, for the first time, a mechanochemical amorphous-to-crystalline transformation strategy that empowers the ambient synthesis of nine imine-linked COFs with diverse functionalities, topologies, and dimensionalities. This solid-state strategy is facile, fast, eco-friendly, scalable, and universal, offering significant advantages over the traditional solvothermal route. Most notably, this strategy enables the synthesis of a crystalline pyrene-based COF that is otherwise inaccessible through *de novo* mechanosynthesis, underscoring the unique advantage of this approach. To shed light on the structural transformation, a mechanochemical "scrambling" experiment of the model compound reveals the high reversibility of the imine bonds in the solid state, which is pivotal for the error correction during COF recrystallization. Harnessing the efficient amorphous-to-crystalline transformation under mechanochemical conditions, this work establishes a potent post-transformation route to imine COFs, representing a valuable new addition to the synthetic toolkit in COF mechanochemistry. Extending this strategy to COFs beyond imine linkages is currently underway in our laboratory.

## Author contributions

Normanda Brown: writing – original draft; investigation; data curation; formal analysis. Yogendra Nailwal: data curation;

formal analysis. Tyra Blair: investigation; data curation. Ziad Alsudairy: investigation; validation; data curation. Qingsong Zhang: data curation; validation. Krystal Kennedy: data curation. Yi Liu: writing – review & editing; data curation; resources; supervision. Xinle Li: conceptualization; writing – review & editing; supervision; project administration; funding acquisition.

## Conflicts of interest

There are no conflicts to declare.

## Data availability

The data supporting this article have been included as part of the supplementary information (SI). Supplementary information: materials, instrumentation, synthetic procedure of COPs, model compounds, and COFs, scrambling experiment, PXRD, FTIR, TGA, TEM analyses and Tables S1–S7 detailing the screened conditions. See DOI: https://doi.org/10.1039/d5mr00161g.

## Acknowledgements

This research was sponsored by the U.S. Department of Energy Early Career Award (DE-SC0022000), National Science Foundation HBCU-EiR program (DMR-2401504), PREM (DMR-2122147), the PREC program (no. 2216807), ACS Petroleum Research Fund New Direction (PRF # 68683-ND10), and NIH/NIMHD grant #2U54MD007590-38 (Pilot Project 1 to Xinle Li). Part of the work was carried out at the Molecular Foundry as a user project, supported by the Office of Science, Office of Basic Energy Sciences, of the U.S. Department of Energy under Contract No. DE-AC02-05CH11231.

## Notes and references

1 C. S. Diercks and O. M. Yaghi, *Science*, 2017, **355**, eaal1585.
2 Z. Wang, S. Zhang, Y. Chen, Z. Zhang and S. Ma, *Chem. Soc. Rev.*, 2020, **49**, 708.
3 T. Skorjanc, D. Shetty and M. Valant, *ACS Sens.*, 2021, **6**, 1461.
4 J. Li, X. Jing, Q. Li, S. Li, X. Gao, X. Feng and B. Wang, *Chem. Soc. Rev.*, 2020, **49**, 3565.
5 G. Zhang, X. Li, Q. Liao, Y. Liu, K. Xi, W. Huang and X. Jia, *Nat. Commun.*, 2018, **9**, 2785.
6 S. Ge, K. Wei, W. Peng, R. Huang, E. Akinlabi, H. Xia, M. W. Shahzad, X. Zhang, B. B. Xu and J. Jiang, *Chem. Soc. Rev.*, 2024, **53**, 11259.
7 C. Sun, D. Sheng, B. Wang and X. Feng, *Angew. Chem., Int. Ed.*, 2023, **135**, e202303378.
8 Z. Alsudairy, N. Brown, A. Campbell, A. Ambus, B. Brown, K. Smith-Petty and X. Li, *Mater. Chem. Front.*, 2023, **7**, 3298.
9 J. Hu, S. K. Gupta, J. Ozdemir and H. Beyzavi, *ACS Appl. Nano Mater.*, 2020, **3**, 6239.
10 S. J. Lyle, P. J. Waller and O. M. Yaghi, *Trends Chem.*, 2019, **1**, 172.
11 B. J. Smith, A. C. Overholts, N. Hwang and W. R. Dichtel, *Chem. Commun.*, 2016, **52**, 3690.
12 D. Stewart, D. Antypov, M. S. Dyer, M. J. Pitcher, A. P. Katsoulidis, P. A. Chater, F. Blanc and M. J. Rosseinsky, *Nat. Commun.*, 2017, **8**, 1102.
13 Z. Lin, X. Yu, Z. Zhao, N. Ding, C. Wang, K. Hu, Y. Zhu and J. Guo, *Nat. Commun.*, 2025, **16**, 1940.
14 W. Kong, W. Jia, R. Wang, Y. Gong, C. Wang, P. Wu and J. Guo, *Chem. Commun.*, 2019, **55**, 75.
15 Y. Zhai, G. Liu, F. Jin, Y. Zhang, X. Gong, Z. Miao, J. Li, M. Zhang, Y. Cui and L. Zhang, *Angew. Chem., Int. Ed.*, 2019, **58**, 17679.
16 J. Tan, S. Namuangruk, W. Kong, N. Kungwan, J. Guo and C. Wang, *Angew. Chem., Int. Ed.*, 2016, **55**, 13979.
17 Z. Xiong, B. Sun, H. Zou, R. Wang, Q. Fang, Z. Zhang and S. Qiu, *J. Am. Chem. Soc.*, 2022, **144**, 6583.
18 C. Fan, H. Wu, J. Guan, X. You, C. Yang, X. Wang, L. Cao, B. Shi, Q. Peng and Y. Kong, *Angew. Chem., Int. Ed.*, 2021, **60**, 18051.
19 L. Cusin, P. Cieciórski, S. Van Gele, F. Heck, S. Krause, P. W. Majewski, B. V. Lotsch, W. Danowski and P. Samorì, *Nat. Synth.*, 2025, **4**, 632.
20 X. Li, C. Yang, B. Sun, S. Cai, Z. Chen, Y. Lv, J. Zhang and Y. Liu, *J. Mater. Chem. A*, 2020, **8**, 16045.
21 J.-L. Do and T. Friščić, *ACS Cent. Sci.*, 2017, **3**, 13.
22 G.-W. Wang, *Chem. Soc. Rev.*, 2013, **42**, 7668.
23 M. J. Muñoz-Batista, D. Rodriguez-Padron, A. R. Puente-Santiago and R. Luque, *ACS Sustainable Chem. Eng.*, 2018, **6**, 9530.
24 N. R. Rightmire and T. P. Hanusa, *Dalton Trans.*, 2016, **45**, 2352.
25 A. Krusenbaum, S. Grätz, G. T. Tigineh, L. Borchardt and J. G. Kim, *Chem. Soc. Rev.*, 2022, **51**, 2873.
26 B. Szczęśniak, S. Borysiuk, J. Choma and M. Jaroniec, *Mater. Horiz.*, 2020, **7**, 1457.
27 Z. Tegudeer, L. C. Davenport, M. E. Kordesch and W.-Y. Gao, *J. Am. Chem. Soc.*, 2025, **147**, 13522.
28 B. P. Biswal, S. Chandra, S. Kandambeth, B. Lukose, T. Heine and R. Banerjee, *J. Am. Chem. Soc.*, 2013, **135**, 5328.
29 S. T. Emmerling, L. S. Germann, P. A. Julien, I. Moudrakovski, M. Etter, T. Friščić, R. E. Dinnebier and B. V. Lotsch, *Chem*, 2021, **7**, 1639.
30 S. Hutsch, A. Leonard, S. Graetz, M. V. Höfler, T. Gutmann and L. Borchardt, *Angew. Chem., Int. Ed.*, 2024, e202403649.
31 R. Gao, N. Zhong, L. Tong, X. Kou, W. Huang, H. Yang, S. Huang, J. Wu, G. Chen and G. Ouyang, *Cell Rep. Phys. Sci.*, 2022, **3**, 101153.
32 H. Chen, D. Feng, F. Wei, F. Guo and A. K. Cheetham, *Angew. Chem., Int. Ed.*, 2025, **64**, e202415454.
33 N. Brown, Q. Zhang, Z. Alsudairy, C. Dun, Y. Nailwal, A. Campbell, C. Harrod, L. Chen, S. Williams, J. J. Urban, Y. Liu and X. Li, *ACS Sustain. Chem. Eng.*, 2024, **12**, 13535.
34 Y. Nailwal, Q. Zhang, N. Brown, Z. Alsudairy, C. Harrod, M. H. Uddin, F. Akram, J. Li, Y. Liu and X. Li, *Chem. Eur J.*, 2025, **31**, e202500339.
35 E. Hamzehpoor, F. Effaty, T. H. Borchers, R. S. Stein, A. Wahrhaftig-Lewis, X. Ottenwaelder, T. FriŠČiĆ and D. F. Perepichka, *Angew. Chem., Int. Ed.*, 2024, e202404539.

36 S. Karak, S. Kandambeth, B. P. Biswal, H. S. Sasmal, S. Kumar, P. Pachfule and R. Banerjee, *J. Am. Chem. Soc.*, 2017, **139**, 1856.
37 N. Brown, Z. Alsudairy, R. Behera, F. Akram, K. Chen, K. Smith-Petty, B. Motley, S. Williams, W. Huang, C. Ingram and X. Li, *Green Chem.*, 2023, **25**, 6287.
38 Y. Nailwal, B. Baker, Z. Alsudairy, M. El Hariri El Nokab, Q. Zhang, T. Wang, S. Cai, Y. Liu and X. Li, *Green Chem.*, 2025, **27**, 8848.
39 J. Fan, X. Suo, T. Wang, Z. Wang, C.-L. Do-Thanh, S. M. Mahurin, T. Kobayashi, Z. Yang and S. Dai, *J. Mater. Chem. A*, 2022, **10**, 14310.
40 Q. Liao, C. Ke, X. Huang, D. Wang, Q. Han, Y. Zhang, Y. Zhang and K. Xi, *Angew. Chem., Int. Ed.*, 2021, **133**, 1431.
41 K. Wang, X. Qiao, H. Ren, Y. Chen and Z. Zhang, *J. Am. Chem. Soc.*, 2025, **147**, 8063.
42 A. Laemont, G. Matthys, R. Lavendomme and P. Van Der Voort, *Angew. Chem., Int. Ed.*, 2024, **63**, e202412420.
43 X. Li, H. Wang, H. Chen, Q. Zheng, Q. Zhang, H. Mao, Y. Liu, S. Cai, B. Sun and C. Dun, *Chem*, 2020, **6**, 933.
44 D. Zhu and R. Verduzco, *ACS Appl. Mater. Interfaces*, 2020, **12**, 33121.
45 Y. He, X. Lin, Y. Zhou, J. H. Chen, Z. Guo and H. Zhan, *Chem. Mater.*, 2021, **33**, 9413.
46 Z. Alsudairy, N. Brown, C. Yang, S. Cai, F. Akram, A. Ambus, C. Ingram and X. Li, *Precis. Chem.*, 2023, **1**, 233.
47 Y. Peng, Y. Huang, Y. Zhu, B. Chen, L. Wang, Z. Lai, Z. Zhang, M. Zhao, C. Tan and N. Yang, *J. Am. Chem. Soc.*, 2017, **139**, 8698.
48 M. G. Rabbani, A. K. Sekizkardes, Z. Kahveci, T. E. Reich, R. Ding and H. M. El-Kaderi, *Chem. Eur J.*, 2013, **19**, 3324.
49 T.-Y. Zhou, S.-Q. Xu, Q. Wen, Z.-F. Pang and X. Zhao, *J. Am. Chem. Soc.*, 2014, **136**, 15885.
50 F. J. Uribe-Romo, J. R. Hunt, H. Furukawa, C. Klöck, M. O'Keeffe and O. M. Yaghi, *J. Am. Chem. Soc.*, 2009, **131**, 4570.
51 M. H. Gohari, P. Ghamari, E. Hamzehpoor, F. Effaty, T. Friščić and D. F. Perepichka, *Chem. Sci.*, 2025, **16**, 18101.